

X-ray Crystal Structures and the Facile Oxidative (Au–C) Cleavage of the Dimethylaurate(I) and Tetramethylaurate(III) Homologues

Dunming Zhu, Sergey V. Lindeman, and Jay K. Kochi*

Department of Chemistry, University of Houston, Houston, Texas 77204-5641

Received January 25, 1999

Dimethylaurate(I) has been prepared as the crystalline tetrabutylammonium salt for comparison with the known tetramethylaurate(III) analogue. The linear structure of dimethylaurate(I) and the square-planar structure of tetramethylaurate(III) have both been confirmed by X-ray crystallography. One-electron oxidation of dimethylaurate(I) by either ferrocenium or arenediazonium cations produces the metastable dimethylgold(II) intermediate, which can be trapped as the paramagnetic 9,10-phenanthrenequinone (PQ) adduct. Otherwise, dimethylgold(II) is subject to rapid reductive elimination of ethane and affords metallic gold (mirror). The analogous oxidation of tetramethylaurate(III) by ferrocenium, arenediazonium, or nitrosonium cations also proceeds via electron transfer to generate the putative tetramethylgold(IV) intermediate. The highly unstable $(\text{CH}_3)_4\text{Au}^{\text{IV}}$ spontaneously undergoes homolytic cleavage to produce methyl radical and the coordinately unsaturated trimethylgold(III), which can be intercepted by added triphenylphosphine to afford $\text{Me}_3\text{-Au}^{\text{III}}\text{PPh}_3$.

Introduction

Alkylmetalates are conventionally considered as nucleophiles and thus have been widely used as sources of the alkyl anion (R^-) in a variety of alkylation reactions.¹ Anionic alkylmetalates are also good electron donors (owing to the electron-donating property of R^-),² and this property should play an important role in alkyl transfer reactions. Indeed, we recently found that alkylation of pyridinium acceptors by tetramethylborate proceeds via an initial electron transfer to establish the significance of the electron-donor property of tetramethylborate in the formal transfer of an alkyl ligand.³ As such, a question arises as to whether the transition-metal counterparts can behave in a similar manner. Although the mechanistic dichotomy between nucleophilic addition and electron transfer in the alkylcuprate addition to electrophiles has been addressed,⁴ the electron-transfer reactivities of transition-metal alkylmetalates, in general, have been greatly hampered by their thermal instability and air sensitivity. In this

context, our early study⁵ showed that the rapid oxidative decomposition of dimethylaurate(I) and tetramethylaurate(III) by dioxygen afforded ethane and metallic gold; unusual dimethylgold(II) and tetramethylgold(IV) species were proposed as transient intermediates.⁶ In this early study, however, dimethylaurate(I) and tetramethylaurate(III) were both generated in situ, and the fate of dioxygen was not identified. The recent availability of tetramethylaurate(III) as a pure crystalline tetrabutylammonium salt⁷ encouraged us to isolate the pure crystalline dimethylaurate(I) analogue. As a result, we examined the structures of both dimethylaurate(I) and tetramethylaurate(III) by X-ray crystallography and explored the electron-transfer reactivity of these alkylmetalates toward electron acceptors in order to clarify the mechanistic details of the oxidative decomposition. For this study, we chose ferrocenium, decamethylferrocenium, arenediazonium, and nitrosonium cations as electron acceptors, since they are well-known one-electron oxidants and widely used to probe electron-transfer processes.⁸

(1) (a) Posner, G. H. *An Introduction to Synthesis Using Organocopper Reagents*; Wiley: New York, 1980. (b) Lipshutz, B. H.; Sengupta, S. In *Organic Reaction*; Wiley: New York, 1992; Vol. 41, Chapter 2, p 135. (c) Kauffmann, T. *Angew. Chem., Int. Ed. Engl.* **1996**, *35*, 386. (d) Uchiyama, M.; Furumoto, S.; Saito, M.; Kondo, Y.; Sakamoto, T. *J. Am. Chem. Soc.* **1997**, *119*, 11425. (e) Uchiyama, M.; Koike, M.; Kameda, M.; Kondo, Y.; Sakamoto, T. *J. Am. Chem. Soc.* **1996**, *118*, 8733. (f) Harada, T.; Katsuhira, T.; Osada, A.; Iwazaki, K.; Maejima, K.; Oku, A. *J. Am. Chem. Soc.* **1996**, *118*, 11377. (g) McWilliams, J. C.; Armstrong, J. D., II; Zheng, N.; Bhupathy, M.; Volante, R. P.; Reider, P. J. *J. Am. Chem. Soc.* **1996**, *118*, 11970. (h) Hojo, M.; Harada, H.; Ito, H.; Hosomi, A. *J. Am. Chem. Soc.* **1997**, *119*, 5459. (i) Inoue, R.; Shinokubo, H.; Oshima, K. *Tetrahedron Lett.* **1996**, *37*, 5377.

(2) (a) Bockman, T. M.; Kochi, J. K. In *Photosensitization and Photocatalysis Using Inorganic and Organometallic Compounds*; Kalyanasundaram, K., Gratzel, M., Eds.; Kluwer Academic: Dordrecht, The Netherlands, 1993; p 407. (b) Kochi, J. K. *Angew. Chem., Int. Ed. Engl.* **1988**, *27*, 1277.

(3) Zhu, D.; Kochi, J. K. *Organometallics* **1999**, *18*, 161.

(4) (a) House, H. O. *Acc. Chem. Res.* **1976**, *9*, 59. (b) Ullenius, C.; Christenson, B. *Pure Appl. Chem.* **1988**, *60*, 57. (c) Vellekoop, A. S.; Smith, R. A. *J. Am. Chem. Soc.* **1994**, *116*, 2902. (d) Nakamura, E.; Mori, S.; Nakamura, M.; Morokuma, K. *J. Am. Chem. Soc.* **1997**, *119*, 4887. (e) Nakamura, E.; Mori, S.; Morokuma, K. *J. Am. Chem. Soc.* **1997**, *119*, 4900.

(5) Komiya, S.; Albright, T. A.; Hoffmann, R.; Kochi, J. K. *J. Am. Chem. Soc.* **1977**, *99*, 8440.

(6) Dialkylcopper(II) species were also proposed as the metastable intermediates in the oxidative decomposition of dialkylcuprate(I) effected by oxidants such as oxygen, nitrobenzene, copper(II) salts, and benzophenone. However, in these cases, the alkylcuprates were generated in situ and the fate of the various oxidants was unclear: Whitesides, G. M.; San Filippo, J.; Casey, C. P.; Panek, E. J. *J. Am. Chem. Soc.* **1967**, *89*, 5302.

(7) Komiya, S.; Ochiai, S.; Ishizaki, Y. *Inorg. Chem.* **1992**, *31*, 3168.

(8) Connelly, N. G.; Geiger, W. E. *Chem. Rev.* **1996**, *96*, 877.

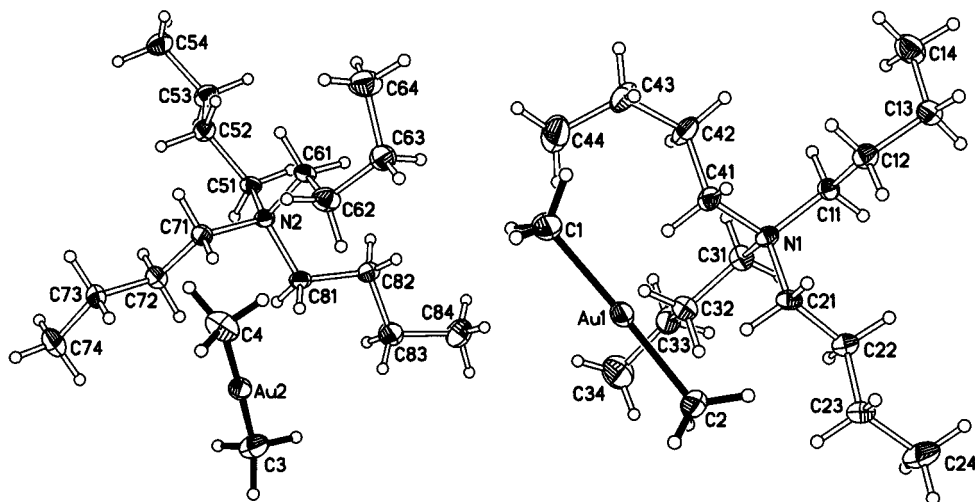


Figure 1. ORTEP diagram of $[N(C_4H_9-n)_4]^+[Au(CH_3)_2]^-$ (thermal ellipsoids drawn at the 50% level) showing the two symmetrically independent structural units.

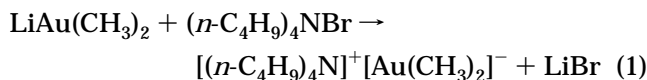
Table 1. Bond Lengths (Å) and Angles (deg) of $Au(CH_3)_2^-$ and $Au(CH_3)_4^-$

$Au(CH_3)_2^-$			
Au(1)–C(1)	2.087(5)	Au(1)–C(2)	2.084(5)
Au(2)–C(3)	2.076(6)	Au(2)–C(4)	2.053(5)
C(1)–Au(1)–C(2)	178.2(2)	C(3)–Au(2)–C(4)	178.2(2)
$Au(CH_3)_4^-$ ^a			
Au(1)–C(1)	2.111(4)	Au(1)–C(2)	2.091(4)
Au(2)–C(3)	2.103(3)	Au(2)–C(4)	2.096(3)
C(1)–Au(1)–C(1')	180.0	C(2)–Au(1)–C(2')	180.0
C(2)–Au(1)–C(1')	88.3(2)	C(2)–Au(1)–C(1)	91.7(2)
C(3)–Au(2)–C(3')	180.0	C(4)–Au(2)–C(4')	180.0
C(4)–Au(2)–C(3)	89.2(1)	C(4)–Au(2)–C(3')	90.8(1)

^a Atoms C(1'), C(2'), C(3'), and C(4') are derived from C(1), C(2), C(3), and C(4), respectively, by corresponding centers of symmetry.

Results and Discussion

Synthesis and X-ray Structures of Dimethylaurate(I) and Tetramethylaurate(III). **Dimethylaurate(I).** Dimethylaurate(I) was prepared as the tetrabutylammonium salt by treatment of $LiAu(CH_3)_2^9$ (generated in situ) with tetrabutylammonium bromide; i.e.



and the crystalline dimethylaurate(I) salt was obtained as colorless needles by the slow diffusion of ether into the THF solution at $-30^\circ C$. The X-ray structure of $[N(C_4H_9)_4][Au(CH_3)_2]$ is shown in Figure 1, and the bond lengths and angles of the dimethylaurate(I) anion are listed in Table 1. There are two symmetrically independent $Au(CH_3)_2^-$ anions having nonequivalent crystalline environments. However, both dimethylaurate(I) moieties have a nearly linear structure with the same C–Au–C bond angle of 178.2° .^{10–12}

(9) (a) Tamaki, A.; Kochi, J. K. *J. Organomet. Chem.* **1973**, *51*, C39. (b) Tamaki, A.; Kochi, J. K. *J. Chem. Soc., Dalton Trans.* **1973**, 2620.

(10) Dimethylaurate(I) and tetramethylaurate(III) have been shown by spectral methods to have linear and square-planar structures, respectively, in accord with other two-coordinate gold(I) and four-coordinate gold(III) complexes: Rice, G. W.; Tobias, R. S. *Inorg. Chem.* **1976**, *15*, 489.

Tetramethylaurate(III). The colorless crystalline tetrabutylammonium salt of tetramethylaurate(III) was obtained as previously described by Komiya and co-workers.⁷ Since the tetrabutylammonium salt of tetramethylaurate(III) was reported to decompose when the crystal was exposed to X-ray irradiation,⁷ we prepared two other crystalline tetramethylaurate(III) salts, $[N(PPH_3)_2][Au(CH_3)_4]$ and $[(PhCH_2)_2N(CH_3)_2][Au(CH_3)_4]$ (see Experimental Section), for X-ray structure analysis. The PPN⁺ salt of tetramethylaurate(III) was recrystallized as colorless needles by the slow diffusion of diethyl ether into the THF solution at $-30^\circ C$, but its X-ray structure was not resolved due to a crystallographic disorder in the anionic moiety. Using the same recrystallization technique, the dibenzylidimethylammonium salt of tetramethylaurate(III) was recrystallized as colorless prisms, and the crystal structure of $[(PhCH_2)_2N(CH_3)_2][Au(CH_3)_4]$ was successfully solved (see Figure 2). The triclinic unit cell contains two cations and two crystallographically centrosymmetric anions. Therefore, the tetramethylaurate(III) anions have an ideal square-planar structure with a slight distortion of bond angles,^{10,13} the C–Au–C bond angles between the cis methyl groups being $88.3(2)$ and $91.7(2)^\circ$ in one anion moiety and $89.17(12)$ and $90.83(12)^\circ$ in the other (Table 1).¹⁴

(11) A few X-ray structures of bis(perfluorophenyl)aurate(I) and bis(alkynyl)aurate(I) are known: (a) Uson, R.; Laguna, A.; Vicente, J.; Garcia, J.; Jones, P. G.; Sheldrick, G. M. *J. Chem. Soc., Dalton Trans.* **1981**, 655. (b) Uson, R.; Laguna, A.; Laguna, M.; Lazaro, I.; Morata, A.; Jones, P. G.; Sheldrick, G. M. *J. Chem. Soc., Dalton Trans.* **1986**, 669. (c) Jones, P. G. *Z. Kristallogr.* **1993**, *208*, 347. (d) Murray, H. H.; Briggs, D. A.; Garzon, G.; Raptis, R. G.; Porter, L. C.; Fackler, J. P., Jr. *Organometallics* **1987**, *6*, 1992. (e) Smith, D. E.; Welch, A. J.; Treurnicht, I.; Puddephatt, R. J. *Inorg. Chem.* **1986**, *25*, 4616. (f) Che, C.-M.; Yip, H.-K.; Lo, W.-C.; Peng, S.-M. *Polyhedron* **1994**, *13*, 887. (g) Vicente, J.; Chicote, M.-T.; Abrisqueta, M.-D.; Jones, P. G. *Organometallics* **1997**, *16*, 5628.

(12) The conformation of methyl groups in dimethylaurate(I) (considering the position of the hydrogen atoms) is eclipsed with the H–C–H angle being about 10° .

(13) Three tetrakis(aryl)aurate(III) salts have been structurally characterized. $Au(C_6H_5)_4^-$: (a) Markwell, A. J. *J. Organomet. Chem.* **1985**, *293*, 257. $Au(C_6F_5)_4^-$: (b) Murray, H. H.; Fackler, J. P., Jr.; Porter, L. C.; Briggs, D. A.; Guerra, M. A.; Lagow, R. J. *Inorg. Chem.* **1987**, *26*, 357. (c) Uson, R.; Laguna, A.; Laguna, M.; Jimenez, J.; Jones, P. G. *Angew. Chem., Int. Ed. Engl.* **1991**, *30*, 198. $Au(C_6Cl_5)_4^-$: (d) Schlueter, J. A.; Geiser, U.; Wang, H. H.; VanZile, M. L.; Fox, S. B.; Williams, J. M.; Laguna, A.; Laguna, M.; Naumann, D.; Roy, T. *Inorg. Chem.* **1997**, *36*, 4265.

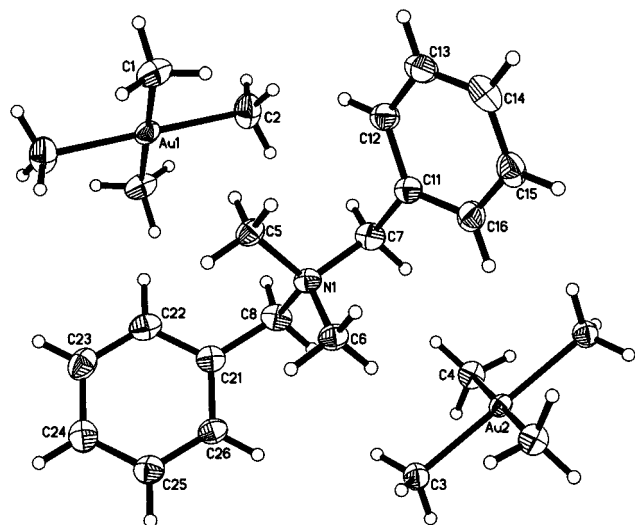


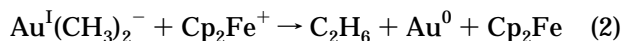
Figure 2. ORTEP diagram of $[(\text{CH}_3)_2\text{N}(\text{CH}_2\text{C}_6\text{H}_5)_2]^+[\text{Au}(\text{CH}_3)_2]^-$ (thermal ellipsoids drawn at the 50% level) showing the ammonium cation and two centrosymmetric anionic moieties. The symmetrically independent atoms are labeled.

Table 2. Oxidation of $\text{Bu}_4\text{N}^+\text{AuMe}_2^-$ with $\text{Cp}_2\text{Fe}^+\text{PF}_6^-$ or $\text{Cp}^*\text{Fe}^+\text{PF}_6^-$ ^a

entry no.	solvent	CH_4	C_2H_6	gold product	$\text{Cp}_2\text{Fe}/\text{Cp}^*\text{Fe}$
1	THF	0.06	0.86	Au (0.97)	0.94
2	CH_3CN	<0.05	0.95	Au (0.96)	0.96
3	THF	0.05	0.88	Au	0.96
4	CH_3CN	<0.05	0.92	Au	0.93
5	THF ^b	0.19	0.18	$\text{Me}_3\text{AuPPh}_3$ (0.34) MeAuPPh_3 (0.40)	0.87
6	CH_3CN ^b	0.10	<0.05	$\text{Me}_3\text{AuPPh}_3$ (0.40) MeAuPPh_3 (0.38)	0.93

^a For entries 1 and 2, $\text{Cp}_2\text{Fe}^+\text{PF}_6^-$ was used as oxidant, while $\text{Cp}^*\text{Fe}^+\text{PF}_6^-$ was used for entries 3–6. The yield was moles of product based on the reactants normalized to 1.0 mol. ^b In the presence of triphenylphosphine.

Oxidatively Induced Reductive Elimination of Dimethylaurate(I). (I) Oxidation with Ferrocenium and Decamethylferrocenium Cations. Oxidation of dimethylaurate(I) with 1 equiv of ferrocenium (or decamethylferrocenium) cation in THF (or acetonitrile) afforded ethane and a gold mirror according to the stoichiometry in eq 2. The ferrocenium (or decameth-



ylferrocenium) cation was reduced to ferrocene (or decamethylferrocene) in quantitative yields, and the results are summarized in Table 2. A mixture of $(\text{CH}_3)_3\text{-AuPPh}_3$ and $\text{CH}_3\text{AuPPh}_3$ in equivalent amounts was obtained when the reactions were carried out in the presence of triphenylphosphine (Table 2).

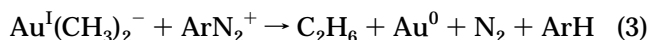
(II) Oxidation with Arenediazonium Cations. The treatment of tetrabutylammonium dimethylaurate(I) with 2,4,6-trichlorobenzenediazonium hexafluorophosphate in THF (or acetonitrile) at -78°C generated ethane and metallic gold according to eq 3, where Ar is

Table 3. Oxidation of Dimethylaurate Anion with Arenediazonium Cations^a

Entry	Ar-	Solvent	CH_4	C_2H_6	N_2	ArH
1		THF	<0.05	0.89	0.94	0.48
2	"	CH_3CN	0.05	0.86	0.96	0.35
3		THF	<0.05	0.89	0.95	0.82
4	"	CH_3CN	<0.05	0.85	0.91	0.56
5		THF	<0.05	0.90	0.98	0.32
6	"	CH_3CN	<0.05	0.83	0.90	0.29
7		THF	<0.05	0.91	0.93	0.47
8	"	CH_3CN	<0.05	0.80	0.89	0.31
9		THF	0	0.95	0.96	0.50
10	"	CH_3CN	<0.05	0.77	0.91	0.33

^a The yields were moles of products based on the reactants normalized to 1.0 mol.

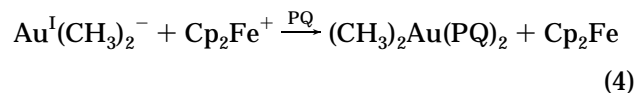
2,4,6- $\text{Cl}_3\text{C}_6\text{H}_2$, *p*- ClC_6H_4 , *p*- BrC_6H_4 , *p*- $\text{CF}_3\text{C}_6\text{H}_4$, or *p*- $\text{CH}_3\text{OC}_6\text{H}_4$. Furthermore, the 2,4,6-trichlorobenzene-



diazonium cation was reduced to 1,3,5-trichlorobenzene with the evolution of nitrogen gas. The oxidation of dimethylaurate(I) with the other arenediazonium cations afforded similar results, as summarized in Table 3.

(III) Electrochemical Oxidation. The cyclic voltammogram of tetrabutylammonium dimethylaurate(I) showed an irreversible anodic wave at $E_p = 98$ mV (vs SCE) at a scan rate of $v = 100$ mV s^{-1} . No reduction wave was observed during the reverse scan, and metallic gold was plated onto the surface of the platinum electrode. The latter suggested that dimethylgold(II) was generated but rapidly decomposed to ethane and gold(0) on the CV time scale (compare eqs 2 and 3).

(IV) Trapping of Dimethylgold(II). The interception of the dimethylgold(II) intermediate was carried out with 9,10-phenanthrenequinone (PQ) as the trapping agent¹⁵ using ferrocenium cation as the oxidant.¹⁸ When dimethylaurate(I) was treated with ferrocenium cation in the presence of 4 equiv of 9,10-phenanthrenequinone, a dark green solution was obtained immediately.¹⁹ A metastable green solid was isolated from the reaction mixture (see Experimental Section) and found to be stable at -78°C . It decomposed at room temperature to yield a mixture of ethane, gold(0), and phenanthrenequinone in the molar ratio of 1:1:2.²⁰ Ferrocenium cation was quantitatively reduced to ferrocene; i.e.



The ESR spectrum of the green bis-PQ adduct ($g =$

(14) The tetramethylaurate(III) anion is centrosymmetric, and the conformations of the trans methyl groups (considering the positions of the hydrogen atoms) are staggered.

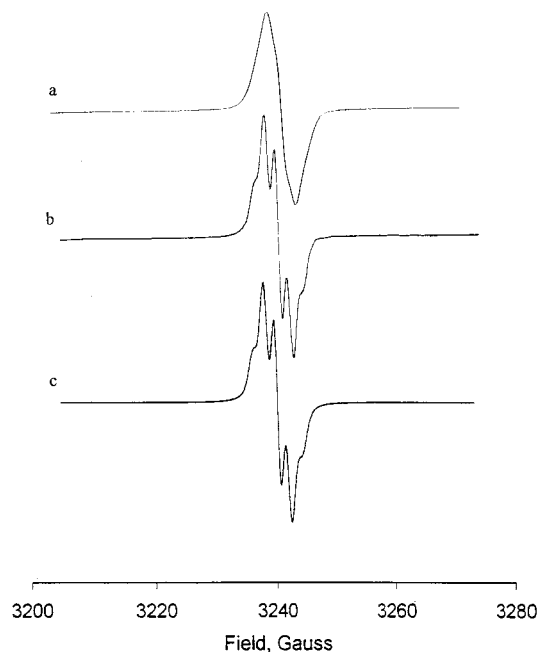


Figure 3. Experimental (a, room temperature; b, $-80\text{ }^{\circ}\text{C}$) and simulated (c) ESR spectra of the adduct $(\text{CH}_3)_2\text{Au}(\text{PQ})_2$. The parameters used for simulation are as follows: the hyperfine splitting constants of the two groups of H atoms of 9,10-phenanthrenequinone and ^{197}Au are 1.75, 0.45, and 0.30 G, respectively; the line width is 0.60 G.

2.0002) measured in THF solution at $-80\text{ }^{\circ}\text{C}$ and the simulated ESR spectrum are shown in Figure 3.²¹ The very weak (unresolved) coupling with ^{197}Au ²² suggests the unpaired electron to be primarily localized on the 9,10-phenanthrenequinone ligand (i.e. as $\text{PQ}^{\bullet-}$).^{16,17} The green adduct can thus be structurally assigned as $(\text{CH}_3)_2\text{Au}^+(\text{PQ}^{\bullet-})(\text{PQ})$. Further support for this assignment is provided by the UV-vis spectrum in Figure 4, which shows the broad band at 700 nm. This intense absorption band may be assigned to the interligand

(15) 9,10-Phenanthrenequinone was chosen as the trapping agent for the following reasons. First, the previous investigations strongly suggest that mononuclear, paramagnetic gold(II) complexes are formed only when good σ -donor and π -acceptor ligands, such as *N,N*-dialkylidithiocarbamates, maleonitriledithiolate, and phthalocyanine, are used to stabilize the metal center.¹⁶ Second, it is known that phenanthrenequinone can stabilize trimethyltin and triphenyllead via adduct formation, suggesting that it is a chelating ligand with good σ -donor and π -acceptor ability.¹⁷

(16) (a) Vanngard, T.; Akerstrom, S. *Nature* **1959**, *184*, 183. (b) Waters, J. H.; Gray, H. B. *J. Am. Chem. Soc.* **1965**, *87*, 3534. (c) MacCragh, A.; Koski, W. S. *J. Am. Chem. Soc.* **1965**, *87*, 2496. (d) Schlupp, R. L.; Maki, A. H. *Inorg. Chem.* **1974**, *13*, 44. (e) Koley, A. P.; Purohit, S.; Prasad, L. S.; Ghosh, S.; Manoharan, P. T. *Inorg. Chem.* **1992**, *31*, 305.

(17) (a) Mochida, K.; Kochi, J. K.; Chen, K. S.; Wan, J. K. S. *J. Am. Chem. Soc.* **1978**, *100*, 2927. (b) Chen, K. S.; Smith, R. T.; Wan, J. K. S. *Can. J. Chem.* **1978**, *56*, 2503. (c) Pierpont, C. G.; Lange, C. W. *Prog. Inorg. Chem.* **1994**, *41*, 331.

(18) Similar results were obtained when *p*-chlorobenzenediazonium cation was used as the oxidant in the trapping experiment.

(19) To trap the dimethylgold(II) intermediate, at least 2 equiv of 9,10-phenanthrenequinone was required (see Experimental Section).

(20) A small amount of phenanthrenehydroquinone was admixed with the phenanthrenequinone (see Experimental Section).

(21) The hyperfine splittings by 2-, 2'-, 4-, and 4'-H atoms of 9,10-phenanthrenequinone and ^{197}Au were not resolved due to the line broadening, which might have resulted from an electron exchange between the phenanthrenequinone anion radical and the Au center or the unreduced phenanthrenequinone: Wertz, J. E.; Bolton, J. R. *Electron Spin Resonance: Elementary Theory and Practical Applications*; McGraw-Hill: New York, 1972.

(22) Computer simulation indicates that the hyperfine splitting constant by ^{197}Au is ~ 0.3 G.

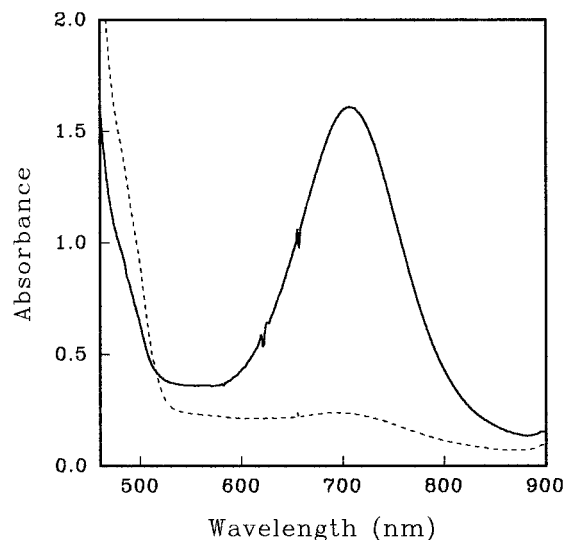


Figure 4. UV-vis spectra of the adduct $(\text{CH}_3)_2\text{Au}(\text{PQ})_2$ in THF solution at $-78\text{ }^{\circ}\text{C}$ (—) and at room temperature (---).

charge-transfer band from the phenanthrenesemiquinone to the phenanthrenequinone ligand.²³ Interligand charge-transfer interactions of this type have been previously observed between the mixed-charge quinone ligands in structurally characterized copper(II) and nickel(I) complexes, i.e., $[(\text{TMEDA})\text{Cu}(\text{PD})(\text{PQ})]$ (TMEDA = tetramethylethylenediamine and PD = 9,10-phenanthrenediolate) and $[\text{LNi}(\text{TCSQ})(\text{TCQ})]$ (L = 2,4,4-trimethyl-1,5,9-triazacyclododec-1-ene, TCSQ = tetrachloro-1,2-benzoquinone, and TCQ = tetrachloro-1,2-benzoquinone).²⁴ Furthermore, as the green solution of the bis-PQ adduct was warmed to room temperature, the 700 nm band bleached (Figure 4) and the hyperfine splittings in the ESR spectrum disappeared (the *g* value did not change; Figure 3a). When the resulting orange solution was immediately recooled to $-78\text{ }^{\circ}\text{C}$, the color of the solution was restored to green; the UV-vis (700 nm) band and the ESR hyperfine splittings appeared concomitantly (although the intensities were somewhat reduced). After a few cycles of this warm/cool process, decomposition was observed, accompanied by the disappearance of the 700 nm absorption band and ESR signal. The bleach of the green color at room temperature could be interpreted by the following equilibrium in solution:

(23) The LMCT character of this absorption band cannot be completely excluded.^{17c} A reviewer suggested $(\text{CH}_3)_2\text{Au}(\text{PQ})_2$ may be a dimer (similar to the dimeric $[(\text{dppn})\text{AuCl}]_2$) in equilibrium with the monomer, implying that the green color resulted from the $\sigma \rightarrow \sigma^*$ transition of the Au-Au bond. This possibility cannot be completely excluded: Yam, V. W.-W.; Choi, S. W.-K.; Cheung, K.-K. *J. Chem. Soc., Chem. Commun.* **1996**, 1173.

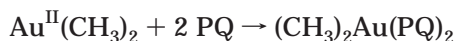
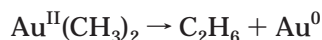
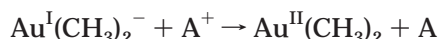
(24) Pierpont et al. reported the X-ray crystal structure of the green complex $(\text{TMEDA})\text{Cu}(\text{PQ})_2$ (TMEDA = tetramethylethylenediamine), in which one of the PQs was identified as 9,10-phenanthrenediolate ligand and the other as the 9,10-phenanthrenequinone ligand. The diolate and quinone ligands were paired together at the metal through a charge-transfer interaction, showing an absorption band at 802 nm: (a) Speier, G.; Tisza, S.; Rockenbauer, A.; Boone, S. R.; Pierpont, C. G. *Inorg. Chem.* **1992**, *31*, 1017. Similarly, $[\text{LNi}(\text{TCQ})_2]$ (L = 2,4,4-trimethyl-1,5,9-triazacyclododec-1-ene and TCQ = 2,3,4,5-tetrachlorobenzoquinone) was structurally characterized as $[\text{LNi}(\text{TCSQ})(\text{TCQ})]$ (TCSQ = tetrachlorosemiquinone), in which the semiquinone and quinone ligands were also paired at the metal through a charge-transfer interaction, showing an intense absorption band at 787 nm: (b) Benelli, C.; Dei, A.; Gatteschi, D.; Pardi, L. *J. Am. Chem. Soc.* **1988**, *110*, 6897.



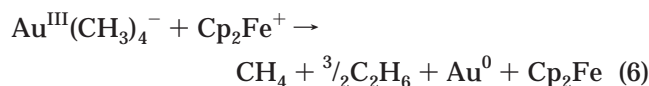
As the temperature increased, the equilibrium shifted to the right side so that the charge-transfer interaction between the phenanthrenequinone anion radical and neutral phenanthrenequinone moieties was not observed. The absence of hyperfine splitting at room temperature was attributed to line broadening²⁵ due to the increased rate of electron exchange between the phenanthrenequinone anion radical and neutral phenanthrenequinone at higher temperature.²⁶

In summary, the oxidation of dimethylaurate(I) with ferrocenium, decamethylferrocenium, or arenediazonium cation proceeds via an initial electron transfer to afford a metastable paramagnetic dimethylgold(II) intermediate. This transient species is subject to facile reductive elimination of ethane to afford a metallic gold mirror.²⁷ Furthermore, the dimethylgold(II) intermediate can be trapped by 9,10-phenanthrenequinone to give the adduct $(\text{CH}_3)_2\text{Au}(\text{PQ})_2$, as shown in Scheme 1, where A^+ is ferrocenium, decamethylferrocenium, or arenediazonium cation and PQ is 9,10-phenanthrenequinone.

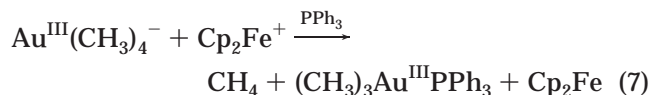
Scheme 1



Oxidatively Induced Homolytic Cleavage of Tetramethylaurate(III). (I) Oxidation with Ferrocenium Cation. The oxidation of tetramethylaurate(III) with 1 equiv of ferrocenium cation in THF (or acetonitrile) generated methane, ethane, and gold metal, according to the stoichiometry in eq 6.²⁸ Ferrocenium



cation was reduced to ferrocene in quantitative yield (Table 4). When the oxidation of tetramethylaurate(III) was carried out in the presence of triphenylphosphine, methane and $(\text{CH}_3)_3\text{Au}^{\text{III}}\text{PPh}_3$ were obtained in equivalent amounts; i.e.



This indicated that the trimethylgold(III) was generated, and it could be intercepted by triphenylphosphine. (Note that the decomposition of trimethylgold(III) yields gold and ethane in a 2:3 molar ratio.) When the oxidation of tetramethylaurate(III) in acetonitrile was

(25) An ESR spectrum identical with that in Figure 3a was obtained by simulation using the same splitting parameters (Figure 3c) and a line width of 1.30 G. In addition, a progressive line broadening was observed by gradually increasing the temperature.

(26) Ward, R. L.; Weissmann, S. I. *J. Am. Chem. Soc.* **1957**, *79*, 2086.

(27) A similar reductive elimination of a pair of alkyl ligands is observed in the two-electron oxidation of dialkyliron(II) complexes. See: Lau, W.; Huffman, J. C.; Kochi, J. K. *Organometallics* **1982**, *1*, 155.

(28) This is different from the reaction of lithium tetramethylaurate with oxygen, in which 2 equiv of ethane and gold metal was produced.⁵

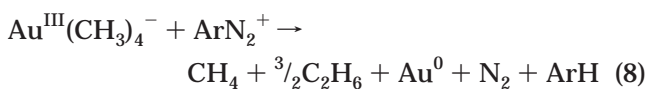
Table 4. Oxidation of $\text{Bu}_4\text{N}^+\text{AuMe}_4^-$ with $\text{Cp}_2\text{Fe}^+\text{PF}_6^-$ ^a

entry no.	solvent	CH_4	C_2H_6	gold product	Cp_2Fe
1	THF	0.91	1.36	Au (0.95)	0.94
2	THF	0.87	0	$\text{Me}_3\text{AuPPh}_3$ (0.98)	0.98
3	Et_2O^b	0.95	<0.05	$\text{Me}_3\text{AuPPh}_3$ (0.94)	0.95
4	CH_3CN	0.83	1.41	Au (0.98)	0.92
5	CH_3CN^b	0.97	0	$\text{Me}_3\text{AuPPh}_3$ (0.89)	0.94

^a The yield was moles of product based on the reactants normalized to 1.0 mol. ^b In the presence of triphenylphosphine.

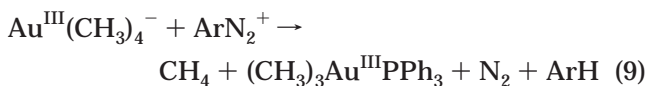
carried out at -40°C , 1 equiv of methane was evolved but no ethane was detectable at this low temperature. One and a half equivalents of ethane were produced when the reaction mixture was warmed to room temperature. The stepwise evolution of methane and ethane suggested that acetonitrile stabilized the coordinatively unsaturated trimethylgold(III) at low temperature. Under the same conditions, tetramethylaurate(III) did not react with decamethylferrocenium cation (which is not unexpected if one considers the lower reduction potential of decamethylferrocenium cation⁸).

(II) Oxidation with Arenediazonium Cations. Oxidation of tetramethylaurate(III) with 2,4,6-trichlorobenzene-diazonium cation in THF (or acetonitrile) at -78°C afforded methane, ethane, and gold according to the stoichiometry in eq 8.²⁸ Concomitantly, the 2,4,6-trichlorobenzene-diazonium cation was reduced to 1,3,5-trichlorobenzene with the evolution of nitrogen gas; i.e.



where Ar is 2,4,6- $\text{Cl}_3\text{C}_6\text{H}_2$, *p*- ClC_6H_4 , *p*- BrC_6H_4 , *p*- $\text{CF}_3\text{C}_6\text{H}_4$, or *p*- $\text{CH}_3\text{OC}_6\text{H}_4$. Oxidation of tetramethylaurate(III) with the other arenediazonium cations (Table 5) followed the same stoichiometry as formulated in eq 8.

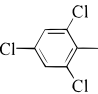
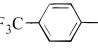
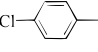
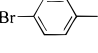
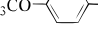
When tetramethylaurate(III) as its tetrabutylammonium salt was treated with 1 equiv of 4-chlorobenzene-diazonium hexafluorophosphate in the presence of triphenylphosphine, a mixture of methane and dinitrogen was found in the gas phase in 92% and 96% yields, respectively; $(\text{CH}_3)_3\text{Au}^{\text{III}}\text{PPh}_3$ was isolated in 91% yield from the solution (eq 9).



(III) Oxidation with Nitrosonium Cation. Upon addition of tetramethylaurate(III) as its tetrabutylammonium salt to the brown solution of $[\text{NO}^+, \text{HMB}]\text{BF}_4^-$ in acetonitrile,²⁹ the solution rapidly bleached and a gold mirror formed within a few minutes. A mixture of methane, ethane, and nitric oxide in a 2:3:2 molar ratio

(29) The uncomplexed nitrosonium cation is such a strong oxidant that the reaction with tetramethylaurate was very complicated. Since nitrosonium interacts with arenes such as hexamethylbenzene to form electron donor-acceptor (EDA) complexes, whose reduction potentials were lower than that of the uncomplexed NO^+ ion, the brown solution of the EDA complex $[\text{NO}^+, \text{HMB}]\text{BF}_4^-$ was used: (a) Kim, E. K.; Kochi, J. K. *J. Am. Chem. Soc.* **1991**, *113*, 4962. (b) Lee, K. Y.; Kuchynka, D. J.; Kochi, J. K. *Inorg. Chem.* **1990**, *29*, 4196.

Table 5. Oxidation of Tetramethylaurate Anion with Arenediazonium Cations^a

Entry	Ar-	Solvent	CH ₄	C ₂ H ₆	N ₂	ArH
1		THF	0.91	1.37	0.94	0.54
2	"	CH ₃ CN	0.88	1.42	0.94	0.35
3		THF	0.82	1.40	0.93	0.63
4	"	CH ₃ CN	0.87	1.39	0.89	0.45
5		THF	0.86	1.39	0.90	0.42
6	"	CH ₃ CN	0.87	1.41	0.94	0.31
7		THF	0.91	1.42	0.93	0.45
8	"	CH ₃ CN	0.83	1.37	0.90	0.31
9		THF	0.93	1.40	0.95	0.48
10	"	CH ₃ CN	0.87	1.38	0.89	0.25

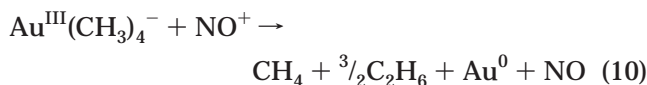
^a The yields were moles of products based on the reactants normalized to 1.0 mol.

Table 6. Oxidation of Bu₄N⁺AuMe₄⁻ with the EDA Complex [NO⁺, HMB]BF₄⁻ in CH₃CN^a

entry no.	CH ₄	C ₂ H ₆ ^a	gold product	NO
1	0.94	1.41	Au	0.96
2 ^b	0.91	0	Me ₃ AuPPh ₃ (0.94)	0.96

^a The yield was moles of product based on the reactants normalized to 1.0 mol. ^b In the presence of triphenylphosphine.

was produced concomitantly; i.e.



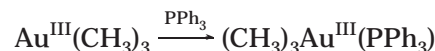
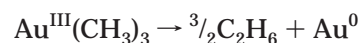
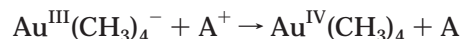
When the same oxidation was performed in the presence of triphenylphosphine, a mixture of methane and (CH₃)₃Au^{III}PPh₃ in equivalent amounts was obtained in high yields, as shown in Table 6.

(IV) Electrochemical Oxidation. The cyclic voltammogram of tetramethylaurate(III) (as its tetrabutylammonium salt) showed an irreversible anodic wave with $E_p = 422$ mV (vs SCE) at a scan rate of $\nu = 100$ mV s⁻¹. No reduction wave was observed during the reverse scan, and metallic gold was plated onto the surface of the platinum electrode. In the presence of triphenylphosphine, an additional irreversible anodic wave appeared at $E_p = 1.32$ V. By comparison with the CV behavior of an authentic sample of (CH₃)₃Au^{III}PPh₃, the electrode process at $E_p = 1.32$ V could be assigned to the anodic oxidation of (CH₃)₃Au^{III}PPh₃. This suggested that the highly unstable tetramethylgold(IV) was produced, but it spontaneously decomposed to generate trimethylgold(III), which was trapped by triphenylphosphine to afford (CH₃)₃Au^{III}PPh₃—all on the CV time scale.

Since ferrocenium, arenediazonium, and nitrosonium cations are well-known one-electron oxidants, they

provide powerful probes for the study of electron-transfer processes. The established complete stoichiometry in eqs 6–10 strongly suggests that the oxidation of tetramethylaurate(III) by ferrocenium, arenediazonium, or nitrosonium cation proceeds via an initial electron transfer to generate the putative tetramethylgold(IV) intermediate in Scheme 2, where A⁺ is ferrocenium, arenediazonium, or nitrosonium cation.³⁰ Ready interception of trimethylgold(III) by triphenylphosphine in chemical and electrochemical oxidations (eqs 7 and 9) implies that the highly unstable tetramethylgold(IV) intermediate spontaneously ruptures to give methyl radical and trimethylgold(III) via the homolytic cleavage of the Au–C bond.³¹ The former abstracts a hydrogen atom from the hydrogen-donor solvent to give methane, and the latter is intercepted by triphenylphosphine to afford the stable (CH₃)₃Au^{III}PPh₃.⁵ In the absence of trapping agent (PPh₃), the coordinately unsaturated trimethylgold(III) rapidly decomposes to generate ethane and gold via reductive elimination, according to the well-established decomposition pathway of trimethylgold(III).³²

Scheme 2



It should be noted that, in our early study, tetramethylaurate(III) was reported to react with dioxygen to afford 2 equiv of ethane and gold metal.⁵ Thus, the evolution of methane and ethane in a 2:3 molar ratio in our present study of the oxidation of tetramethylaurate(III) suggests that the reaction of tetramethylaurate(III) with dioxygen may not be a single electron-transfer process to produce a tetramethylgold(IV) intermediate and that dioxygen may not necessarily act only as a one-electron oxidant.

Conclusion

Dimethylaurate(I) and tetramethylaurate(III) can be isolated as pure crystalline tetrabutylammonium salts, and their electron-transfer reactivities toward electron acceptors have been examined. One-electron oxidation of dimethylaurate(I) produces the metastable dimethylgold(II). This intermediate can be trapped by 9,10-phenanthrenequinone as the adduct (CH₃)₂Au(PQ)₂, or it decomposes via facile reductive elimination to ethane and metallic gold mirror. Analogously, the oxidation of tetramethylaurate(III) generates the putative tetram-

(30) Tetramethylgold(IV) is highly transient, and all attempts to trap it were unsuccessful.

(31) A similar homolytic cleavage of an alkyl ligand is observed in the one-electron oxidation of dimethylmercury(II). See: Chen, J. Y.; Gardner, H. C.; Kochi, J. K. *J. Am. Chem. Soc.* **1976**, *98*, 6150.

(32) It has been established that trimethylgold(III) decomposes to ethane and methylgold(I) via reductive elimination. The latter further decomposes to ethane and gold: (a) Komiyama, S.; Albright, T. A.; Hoffmann, R.; Kochi, J. K. *J. Am. Chem. Soc.* **1976**, *98*, 7255. (b) Tamaki, A.; Magennis, S. A.; Kochi, J. K. *J. Am. Chem. Soc.* **1974**, *96*, 6140.

ethylgold(IV) intermediate. In contrast to dimethylgold(II), the highly unstable tetramethylgold(IV) undergoes rapid homolytic cleavage to produce methyl radical and trimethylgold(III). The latter can be intercepted by triphenylphosphine to afford $\text{Me}_3\text{Au}^{\text{III}}\text{PPh}_3$. We hope theoretical analysis will shed some light on the reason for the different cleavage modes of the Au–C bonds in tetramethylgold(IV) and dimethylgold(II) intermediates.

Experimental Section

All manipulations were carried out under argon or helium atmosphere using standard Schlenk techniques or gloveboxes. Solvents such as ether, THF, benzene, and pentane were dried over sodium benzophenone ketyl and distilled and stored under argon before use. Acetonitrile was treated with KMnO_4 (1 g/L) and refluxed for 1 h. The distilled acetonitrile was then refluxed over P_2O_5 and CaH_2 , respectively, and distilled and stored under argon. Methylithium (1.4 M solution in ether), iodomethane, and phenanthrenequinone were used as received. Triphenylphosphine, tetrabutylammonium bromide, dibenzylidimethylammonium chloride, and $\text{Cp}_2\text{Fe}^+\text{PF}_6^-$ were recrystallized from the appropriate solvents. MeAuPPh_3 ,³³ $\text{Me}_3\text{AuPPh}_3$,^{9b} $[\text{NBU}_4][\text{AuMe}_4]$,⁷ $\text{Cp}^*\text{Fe}^+\text{BF}_4^-$,³⁴ and arenediazonium salts³⁵ were prepared by the published methods. No special precaution was exercised (with regard to light sensitivity) in the handling of these methylaurates. The hydrocarbon gases were analyzed by gas chromatography using a Gow-Mac 550 gas chromatograph equipped with a thermal conductivity detector and a 2 ft Porapak Q column. Quantitative analysis was performed by the internal standard (ethylene) method after calibration under reaction conditions. The methylgold products were analyzed by ^1H NMR using toluene as the internal standard. Elemental analyses were conducted by Atlantic Microlab Inc. UV–visible spectra were measured on a Hewlett-Packard 8450A diode-array spectrometer. ^1H and ^{13}C NMR spectra were recorded on a General Electric QE-300 spectrometer. ESR spectra were recorded on a Varian E-Line Century Series EPR spectrometer. Cyclic voltammetry was performed on a BAS 100A electrochemical analyzer using (*n*-Bu) $_4\text{N}^+\text{PF}_6^-$ (0.1 M) as supporting electrolyte.

Synthesis of $[\text{N}(\text{C}_4\text{H}_9-n)_4][\text{Au}(\text{CH}_3)_2]$. An ether solution of $\text{LiAu}(\text{CH}_3)_2$ (1.40 mmol) was prepared by treating $\text{CH}_3\text{-AuPPh}_3$ (0.65 g, 1.40 mmol) with methylithium (1.40 mmol) at 0 °C.⁹ To this solution was added a solution of $[\text{N}(\text{C}_4\text{H}_9-n)_4]\text{-Br}$ (0.45 g, 1.40 mmol) in 50 mL of benzene. After the reaction mixture was stirred overnight at room temperature, the solvent was removed and the residue was extracted with benzene (2 × 40 mL). Removal of the solvent from the combined benzene extracts afforded a white solid, which was washed with pentane and recrystallized by slow diffusion of diethyl ether into the THF solution to give $[\text{N}(\text{C}_4\text{H}_9-n)_4][\text{Au}(\text{CH}_3)_2]$ as colorless needlelike crystals (0.52 g, 78% yield). Anal. Calcd for $\text{C}_{18}\text{H}_{42}\text{NAu}$: C, 46.05; H, 9.02; N, 2.98. Found: C, 46.30; H, 8.98; N, 3.00. ^1H NMR (C_6D_6 ; δ (ppm)): 0.329 (s, 6H, Au–CH₃), 0.951 (t, *J* = 7.2 Hz, 12H, CH₂), 1.398 (m, 8H, CH₂), 1.497 (m, 8H, CH₂), 3.278 (t, *J* = 7.5 Hz, 8H, CH₂). ^{13}C NMR (C_6D_6 ; δ (ppm)): 10.837 (Au–CH₃), 13.670 (CH₃), 19.753 (CH₂), 24.096 (CH₂), 58.433 (CH₂).

Synthesis of $[\text{N}(\text{PPh}_3)_2][\text{Au}(\text{CH}_3)_4]$. An ether solution of $\text{LiAu}(\text{CH}_3)_4$ (0.85 mmol) was prepared by treating $(\text{CH}_3)_3\text{-AuPPh}_3$ (0.427 g, 0.85 mmol) with methylithium (0.85 mmol)

at 0 °C.³⁶ To this solution were added $[\text{N}(\text{PPh}_3)_2]\text{Cl}$ (487 mg, 0.85 mmol) and 30 mL of THF. The reaction mixture was stirred overnight at room temperature. Workup similar to that described above gave $[\text{N}(\text{PPh}_3)_2][\text{Au}(\text{CH}_3)_4]$ as colorless needlelike crystals (0.375 g, 55% yield). Anal. Calcd for $\text{C}_{40}\text{H}_{42}\text{NP}_2\text{-Au}$: C, 60.38; H, 5.32; N, 1.76. Found: C, 60.08; H, 5.29; N, 1.98. ^1H NMR (THF-*d*₆; δ (ppm)): –0.312 (s, 12H, Au–CH₃), 7.4–7.9 (m, 30H, C₆H₅).

Synthesis of $[\text{N}(\text{CH}_3)_2(\text{CH}_2\text{C}_6\text{H}_5)_2][\text{Au}(\text{CH}_3)_4]$. A procedure similar to that described above was followed, and $[\text{N}(\text{CH}_3)_2(\text{CH}_2\text{C}_6\text{H}_5)_2][\text{Au}(\text{CH}_3)_4]$ was obtained as colorless prismatic crystals (52% yield). Anal. Calcd for $\text{C}_{20}\text{H}_{32}\text{NAu}$: C, 49.68; H, 6.67; N, 2.90. Found: C, 49.54; H, 6.62; N, 3.01. ^1H NMR (THF-*d*₆; δ (ppm)): –0.084 (s, 12H, Au–CH₃), 3.06 (s, 6H, CH₃), 4.741 (s, 4H, CH₂), 7.509 (m, 6H, Ar–H), 7.643 (m, 4H, Ar–H).

General Procedure for the Oxidations of Dimethylaurate(I) and Tetramethylaurate(III). Oxidation of tetrabutylammonium dimethylaurate(I) with ferrocenium hexafluorophosphate is used as an example and described as follows. To a frozen solution of $[\text{N}(\text{C}_4\text{H}_9-n)_4][\text{Au}(\text{CH}_3)_2]$ (47 mg, 0.1 mmol) in 10 mL of THF at –196 °C was added $\text{Cp}_2\text{Fe}^+\text{PF}_6^-$ (33 mg, 0.1 mmol) under a helium atmosphere. The reaction flask was then sealed with a rubber septum and warmed to room temperature. During this period, the reaction mixture turned to an orange solution and a gold mirror formed concomitantly. At this point, 0.1 mmol of ethylene was added into the flask as an internal standard via a gastight syringe. The gas phase was then analyzed by gas chromatography to determine the yield of methane and ethane. The solvent was removed, the residue was dissolved in CDCl_3 , and 0.1 mmol of toluene was added to serve as internal standard. The yield of ferrocene was determined by ^1H NMR. The yield of gold metal was determined gravimetrically by digesting the samples in concentrated sulfuric acid. In the cases of arenediazonium cations as the oxidant, the reaction mixture was quenched with water and extracted with ether. The ether extract was dried over anhydrous Na_2SO_4 and analyzed by GC and GC-MS to determine the yields of arenes. The results are summarized in Tables 2–6.

Trapping of Dimethylgold(II) with 9,10-Phenanthrenequinone. (I) One Equivalent of 9,10-Phenanthrenequinone. 9,10-Phenanthrenequinone (21.0 mg, 0.10 mmol) was added to a tetrahydrofuran solution of $[\text{N}(\text{C}_4\text{H}_9-n)_4][\text{Au}(\text{CH}_3)_2]$ (47.0 mg, 0.10 mmol) at –78 °C. To the resulting orange solution was added $\text{Cp}_2\text{Fe}^+\text{PF}_6^-$ (33.1 mg, 0.10 mmol) at –78 °C. The mixture was stirred at this temperature until $\text{Cp}_2\text{Fe}^+\text{PF}_6^-$ dissolved to give an orange solution. Ethane was produced in 97% yield, as determined by GC analysis of the gas phase.

(II) Two Equivalents of 9,10-Phenanthrenequinone. 9,10-Phenanthrenequinone (41.6 mg, 0.20 mmol) was added to a tetrahydrofuran solution of $[\text{N}(\text{C}_4\text{H}_9-n)_4][\text{Au}(\text{CH}_3)_2]$ (46.8 mg, 0.10 mmol) at –78 °C. To the resulting orange solution was added $\text{Cp}_2\text{Fe}^+\text{PF}_6^-$ (33.1 mg, 0.10 mmol) at –78 °C. The mixture was stirred at this temperature until $\text{Cp}_2\text{Fe}^+\text{PF}_6^-$ dissolved to give a dark green solution. A 1.0 mL portion of this solution was withdrawn via a gastight syringe and diluted with 1 mL of THF at –78 °C. The UV–vis spectrum of the dilute solution was measured at –78 °C, and a broad band at about 700 nm was observed. The gas phase was analyzed by gas chromatography, and no methane or ethane was observed. The reaction mixture was then warmed to room temperature. The dark green solution turned to orange, and a black precipitate formed. The orange solution showed neither the 700 nm band nor an ESR signal. GC analysis of the gas phase indicated that ethane was evolved in 95% yield.

(33) Coates, G. E.; Parkin, S. *J. Chem. Soc.* **1962**, 3220.
(34) Miller, J. S.; Calabrese, J. C.; Rommelmann, H.; Chittipeddi, S. R.; Zhang, J. H.; Reiff, W. M.; Epstein, A. J. *J. Am. Chem. Soc.* **1987**, *109*, 769.

(35) Roe, A. *Org. React.* **1949**, *5*, 193.

(36) (a) Rice, G. W.; Tobias, R. S. *Inorg. Chem.* **1975**, *14*, 2402. (b) Komiya, S.; Ozaki, S.; Endo, I.; Inoue, K.; Kasuga, N.; Ishizaki, Y. *J. Organomet. Chem.* **1992**, *433*, 337. (c) Komiya, S.; Endo, I.; Ozaki, S.; Ishizaki, Y. *Chem. Lett.* **1988**, 63.

(III) Four Equivalent of 9,10-Phenanthrenequinone.

9,10-Phenanthrenequinone (125.0 mg, 0.60 mmol) was added to a tetrahydrofuran solution of $[\text{N}(\text{C}_4\text{H}_9-n)_4][\text{Au}(\text{CH}_3)_2]$ (70.5 mg, 0.15 mmol) at -78°C . To the resulting orange solution was added $\text{Cp}_2\text{Fe}^+\text{PF}_6^-$ (50.0 mg, 0.15 mmol) at -78°C . The mixture was stirred at this temperature until $\text{Cp}_2\text{Fe}^+\text{PF}_6^-$ dissolved to give a dark green solution. A 1.0 mL portion of the solution was withdrawn via a gastight syringe and diluted with THF at -78°C . The UV-vis spectrum of the dilute solution was measured at -78°C , and a broad band at about 700 nm was observed. The gas phase was analyzed by gas chromatography, and no methane or ethane was observed. An ESR sample was prepared at -78°C , and the ESR spectrum was measured at -80°C . In another run of this experiment, the reaction mixture was kept at -78°C for 1 day and a green precipitate formed. The solvent was removed via a syringe to give a green solid in about 70% yield, but attempts to obtain crystalline material were unsuccessful. The green solid was dissolved in THF at -78°C , and its UV-vis and ESR spectra were measured at -78 and -80°C , respectively. The green solid turned to black upon being warmed to room temperature. Analysis of the gas phase indicated that 0.93 equiv of ethane was evolved and no methane was detected. The residue was dissolved in THF to give an orange solution and a black solid. The orange solution was characterized by GC and GC-MS to contain 1.57 equiv of 9,10-phenanthrenequinone and 0.42 equiv of phenanthrenehydroquinone. The black solid was identified as gold metal (about 1.0 equiv).

Trapping of Trimethylgold(III) with PPh_3 . To a frozen THF solution containing $[\text{N}(\text{C}_4\text{H}_9-n)_4][\text{Au}(\text{CH}_3)_4]$ (50.4 mg, 0.1 mmol) and triphenylphosphine (26.2 mg, 0.1 mmol) at -196°C was added $\text{Cp}_2\text{Fe}^+\text{PF}_6^-$ (33 mg, 0.1 mmol) under a helium atmosphere. The reaction flask was then sealed with a rubber septum and warmed to room temperature. The reaction mixture turned to an orange solution. The gas analysis indicated that 0.087 mmol of methane was evolved, but no ethane was detected. The solvent was removed, and the residue was dissolved in CDCl_3 . ^1H NMR analysis indicated that 0.098 mmol of Cp_2Fe and 0.098 mmol of $(\text{CH}_3)_3\text{AuPPh}_3$ were produced. $(\text{CH}_3)_3\text{AuPPh}_3$ was identified by ^1H NMR: δ 0.03 ppm ($J = 7$ Hz) for cis CH_3 , 1.1 ppm ($J = 9$ Hz) for trans CH_3 .

X-ray Crystallography.³⁷ The cell dimensions and diffraction intensities of $[\text{N}(\text{C}_4\text{H}_9-n)_4][\text{Au}(\text{CH}_3)_2]$ and $[\text{N}(\text{CH}_3)_2(\text{CH}_2\text{C}_6\text{H}_5)_2][\text{Au}(\text{CH}_3)_4]$ were measured at -150°C with a Siemens SMART diffractometer equipped with a CCD detector and an LT-2 low-temperature device. The data were collected with graphite-monochromated Mo $K\alpha$ radiation ($\lambda = 0.71073$ Å) using the ω -scan technique over a hemisphere of the reciprocal space. The usual Lorentz and polarization corrections were made. The decay and extinction corrections have been considered to be negligible for the crystals investigated. Absorption correction was done using the SADABS procedure.³⁸ All the structures were solved by direct methods³⁹ and refined by full-matrix least squares on F^2 in anisotropic approximation for all non-hydrogen atoms.⁴⁰ All the hydrogen

(37) Atomic coordinates for the structures of $[\text{N}(\text{C}_4\text{H}_9-n)_4][\text{Au}(\text{CH}_3)_2]$ and $[\text{N}(\text{CH}_3)_2(\text{CH}_2\text{C}_6\text{H}_5)_2][\text{Au}(\text{CH}_3)_4]$ have been deposited with the Cambridge Crystallographic Data Centre. They can be obtained, upon request, from the Director, Cambridge Crystallographic Data Centre, 12 Union Road, Cambridge, CB2 1EZ, U.K.

(38) Sheldrick, G. M. SADABS: Program for Semiempirical Absorption Correction; University of Göttingen, Göttingen, Germany, 1996.

Table 7. Crystallographic Data and Details of Refinements for $[\text{N}(\text{C}_4\text{H}_9-n)_4][\text{Au}(\text{CH}_3)_2]^-$ (1) and $[(\text{CH}_3)_2\text{N}(\text{CH}_2\text{C}_6\text{H}_5)_2][\text{Au}(\text{CH}_3)_4]^-$ (2)

	1	2
formula	$\text{C}_{18}\text{H}_{42}\text{AuN}$	$\text{C}_{20}\text{H}_{32}\text{AuN}$
fw	469.49	483.43
cryst syst	monoclinic	triclinic
space group	$P2_1/n$	$P1$
<i>a</i> , Å	15.9464(1)	8.5946(1)
<i>b</i> , Å	16.0965(2)	10.0649(1)
<i>c</i> , Å	16.2923(2)	12.2762(2)
α , deg	90	86.281(1)
β , deg	96.646(1)	76.216(1)
γ , deg	90	68.936(1)
<i>V</i> , Å ³	4153.83(8)	962.19(2)
<i>Z</i>	8	2
cryst size, mm	$0.4 \times 0.1 \times 0.06$	$0.4 \times 0.35 \times 0.3$
<i>F</i> (000)	1888	476
<i>D_c</i> , g cm ⁻³	1.501	1.669
μ (Mo $K\alpha$), mm ⁻¹	7.078	7.643
2θ range, deg	3.4–72.7	4.4–72.5
<i>h</i> _{min} ; <i>h</i> _{max}	–26; 26	–13; 14
<i>k</i> _{min} ; <i>k</i> _{max}	0; 26	–16; 16
<i>l</i> _{min} ; <i>l</i> _{max}	0; 27	0; 20
no. of measd rflns	52 159	12 050
no. of indep rflns	18 886	8298
<i>R</i> _{int}	0.0815	0.0173
no. of obsd rflns ^a	17 704	8276
total no. of variables	405	208
<i>R</i> ^b ($I > 2\sigma(I)$)	0.0485	0.0255
<i>R</i> _w ^c ($I > 2\sigma(I)$)	0.0842	0.0571
<i>S</i> ^d	0.921	1.111
$\Delta\rho_{\text{max}}/\Delta\rho_{\text{min}}$, e Å ⁻³	2.464/–3.581	1.414/–1.471
Δ scheme coeff ^e (<i>a/b</i>)	0.0333/0	0.0217/1.92

^a With $I > 2.0\sigma(I)$. ^b $R = \sum |F_o| - |F_c| / \sum |F_o|$. ^c $R_w = \{\sum [w(F_o^2 - F_c^2)^2] / \sum [w(F_o^2)]\}^{1/2}$. ^d $S = \{\sum [w(F_o^2 - F_c^2)^2] / \sum (N - n)\}^{1/2}$. ^e $w = 1/[\sigma^2(F_o^2) + (aP)^2 + bP]$, where $P = (F_o^2)/3 + 2(F_c^2)/3$.

atoms in both structures were placed in geometrically calculated positions and refined using a riding/rotating model⁴⁰ with the isotropic temperature factors constrained to be $U_{\text{iso}}(\text{H}) = 1.2U_{\text{eq}}(\text{C})$ of the adjacent carbon atom. Crystal data and refinement details are given in Table 7.

Acknowledgment. We thank T. Dhanasekaran for assistance with ESR measurements and the National Science Foundation and R. A. Welch Foundation for financial support.

Supporting Information Available: Tables and figures giving crystal structure data for $[\text{N}(\text{C}_4\text{H}_9-n)_4][\text{Au}(\text{CH}_3)_2]$ and $[\text{N}(\text{CH}_3)_2(\text{CH}_2\text{C}_6\text{H}_5)_2][\text{Au}(\text{CH}_3)_4]$, including atomic coordinates, anisotropic thermal parameters, bond lengths/angles, hydrogen coordinates, and unit cell and packing diagrams. This material is available free of charge via the Internet at <http://pubs.acs.org>.

OM990043S

(39) Sheldrick, G. M. SHELXS86: Program for the Solution of Crystal Structures; University of Göttingen, Göttingen, Germany, 1985.

(40) Sheldrick, G. M. SHELXL93: Program for the Refinement of Crystal Structures; University of Göttingen, Göttingen, Germany, 1993.